Appl. Phys. B 67, 433–441 (1998)

Applied Physics B
Lasers
and Optics

A tunable diode laser system for the remote sensing of on-road vehicle emissions

D.D. Nelson[1], M.S. Zahniser[1], J.B. McManus[1], C.E. Kolb[1], J.L. Jiménez[2]

[1] Aerodyne Research, Inc., 45 Manning Rd., Billerica, MA 01821-3976, USA
(Fax: +1-978/663-4918, E-mail: ddn@aerodyne.com; E-mail: mz@aerodyne.com; E-mail: mcmanus@aerodyne.com; E-mail: kolb@aerodyne.com)
[2] Massachusetts Institute of Technology, Department of Chemical Engineering, 66-060, Cambridge, MA, 02139, USA
(Fax: +1-617/258-0546, E-mail: jljimene@mit.edu)

Received: 18 May 1998/Revised version: 1 July 1998

Abstract. A tunable infrared laser differential absorption spectrometer (TILDAS) has been developed to measure air-pollutant emission from on-road motor vehicles. The system uses a monostatic source–detector platform and a retro-reflector. It has been shown to be able to measure the emissions from individual vehicles at highway speeds. Excellent detection sensitivity is obtained with measurement precision as small as 3 ppmv of the exhaust under ideal conditions. Long path lengths (100 m or more) can be achieved due to the coherent nature of laser radiation. NO, N_2O, and NO_2 emissions have been measured with this instrument. The system is also capable of measuring CO, NH_3, H_2CO, CH_3OH, and other small molecules in vehicle exhaust.

PACS: 42.68.Kh; 82.80.Ch; 42.55.Px

Public demand for improved air quality drives the need to reduce air-pollutant emissions. Motor vehicles are thought to be the single largest source of many air pollutants in urban areas [1]. However, the exact amounts of air pollutants emitted by motor vehicles are highly uncertain. Many recent studies have found that even the best emission inventory models cannot consistently predict real-world emissions better than within a factor of 2 [1–7]. For these reasons considerable effort has recently been expended to develop instrumentation and measurement techniques which better specify CO, VOC, and NO_x motor vehicle fleet emissions under actual operating conditions [8, 9]. Tunnel studies [2–5] can be used to obtain average fleet emission factors, while ambient air measurements in the vicinity of large roadways [6, 7] can assess the pollutant emission ratios (CO/NO_x and VOC/NO_x). However, neither of these methods can provide information about vehicle-to-vehicle variations in emissions. Although it is possible to fit individual vehicles with on-board instrumentation capable of pollutant monitoring, such instrumentation is necessarily limited to a small number of test vehicles and cannot measure the emissions of non-cooperating vehicles.

Remote sensing instruments using open path spectroscopy can monitor individual vehicle emissions by scaling the pollutant column density to the exhaust carbon dioxide column density measured immediately behind the vehicle. These instruments have the potential to provide the best possible information on the actual in-use emission profiles. By simultaneously capturing a video image of the vehicle's license plate, the distribution of emissions versus vehicle age, vehicle type, or manufacturer can be determined. Remote sensing can also be used as a way to identify high emitters and direct them to inspection and maintenance programs. These actions can lead to more cost-effective improvements in air quality [10, 11].

Non-dispersive infrared (NDIR) instruments to measure CO emissions have been pioneered by the University of Denver [12] and also demonstrated by General Motors [13] and Hughes Santa Barbara Research Center (SBRC) [14]. These three groups have also developed NDIR instruments which measure a portion of the VOC emissions [14–16]. Successful remote sensing measurements of exhaust NO_x emissions from on-road vehicles has been more difficult. Field-proven instruments, based on either NDIR or ultraviolet absorption spectroscopy [14, 17] claim a precision (1σ) of about 300 ppm NO in the exhaust of the vehicle. Since most vehicles are thought to emit less than 300 ppm NO, a more precise instrument than the commercially available ones is needed. Such an instrument would also be advantageous for more precise identification of high-NO emitters. A new ultraviolet-based remote sensor claims a standard deviation of about 20 ppm NO in the exhaust under parking-lot conditions [18], but on-road data have not yet been presented. A gas-filter correlation (GFCR) instrument which claims a potential sensitivity of 10 ppm NO is in the early stages of development [19].

In this paper we describe our tunable infrared laser differential absorption spectroscopy (TILDAS) remote sensing instrument. The TILDAS technique is also known as tunable diode laser (TDL) spectroscopy and tunable diode laser absorption spectroscopy (TDLAS). This instrument can be used to monitor the overwhelming majority of interesting atmospheric species, including CO, NO_2, N_2O, NH_3, CH_2O, and other small-molecule hydrocarbons. Due to its high spectral resolution, the TILDAS instrument is inherently very sensitive and interference free. In addition, the range of the instrument is excellent, allowing measurements of vehicle emissions across several traffic lanes. The primary purpose of its

development has been the measurement of NO emission indices for aircraft engines and for on-road vehicles. Thus, the instrument description, calibration, and performance verification are presented with NO as the target species. The TILDAS instrument represents a major breakthrough with a detection limit for NO of 9 ppm (3σ) of the exhaust, an improvement of approximately a factor of 100 over the two commercial techniques.

This paper is organized as follows. First we describe the application of the TILDAS technique to the remote sensing of air pollutants. Then we describe the construction and operation of the instrument. Finally we present some NO measurement results showing the accuracy and sensitivity of the instrument.

1 Description of the TILDAS trace gas remote sensor

1.1 Principle of measurement

Atmospheric trace gas measurements with tunable diode laser spectroscopy generally use reduced-pressure sampling to take advantage of the narrow line width of the laser source. Tunable diode laser spectroscopy is less frequently used in open-path remote sensing applications [20] although open-path measurements of ambient CO were demonstrated early on by Ku and coworkers [21]. Our TILDAS remote sensing instrument measures vehicle pollutant emissions by sending two overlapping infrared laser beams across the roadway through the exhaust plumes of passing vehicles. The lasers simultaneously measure NO and CO_2 emissions with high detection sensitivity and high temporal resolution. The two-color spectrometer co-aligns two diode laser beams by using a beam splitter (see Fig. 1). The two beams therefore travel the same path and sample identical portions of the exhaust plume. Both lasers are monitored by the same detector upon returning to the optical table. Their signals are distinguished by rapid temporal multiplexing of the lasers so that only one laser is turned on at any given instant. This two-color across-road instrument was constructed with support from the NASA Atmospheric Effects of Aircraft Program (AEAP) for measurements of the exhaust from jet aircraft engines [22, 23].

The use of CO_2 as a reference gas allows one to make quantitative measurements of exhaust species without knowledge of the exhaust plume location or extent of dilution. Since all gases in the exhaust plume are transported together by turbulent diffusion, the ratio of the measured column densities of NO and CO_2 provides an emission index for NO. The emission index is simply the number of NO molecules per CO_2 molecule in the exhaust plume. This is the fundamental quantity measured by this instrument.

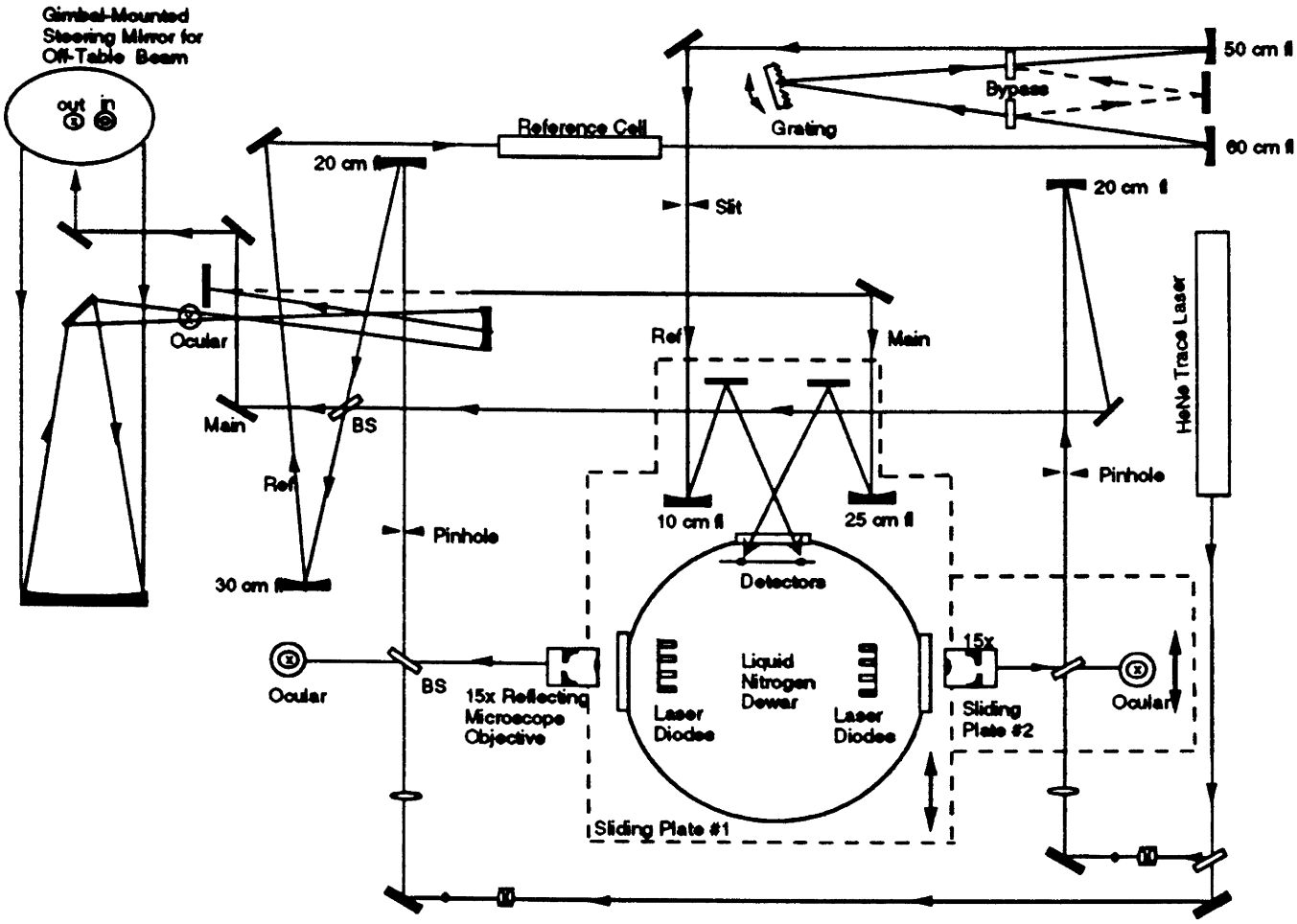

Fig. 1. Optical layout of the TILDAS dual laser instrument

We can use the measured emission index to determine the concentration of NO present in the exhaust of an on-road vehicle. Since the complete combustion of gasoline produces a known CO_2 concentration, one can determine the NO concentration in the exhaust plume of the vehicle (in parts per million meter or ppm-m) in the following manner:

$$[\mathrm{NO}] = \frac{\mathrm{NO(ppm\text{-}m)}}{\mathrm{CO_2(ppm\text{-}m)}}[\mathrm{CO_2}]_\mathrm{s} \quad (1)$$

where $[CO_2]_s$ is the concentration of carbon dioxide produced in the stoichiometric combustion of gasoline. The emission index can be easily converted to units of grams of NO per unit of fuel, which can be used in fuel-based emission inventories [24].

If a vehicle produces a large concentration of CO, the above expression will overestimate the NO concentration. This is not usually a significant problem, but if the CO concentration were also measured, the emission index could be corrected for this [25]. For example, the above formula would overestimate the NO concentration by only 2.9% (on average) for 822 cars for which NO, CO_2, and CO were measured simultaneously using a TILDAS and an NDIR instrument [27, 28]. A four-laser TILDAS instrument under development at Aerodyne Research will allow the measurement of at least four species simultaneously and will therefore eliminate this difficulty by monitoring NO, CO_2, and CO simultaneously.

1.2 Optical layout of the instrument

The optical module of the instrument is shown in Fig. 1. It is designed to be compact, a design which is facilitated by using a liquid-nitrogen dewar that contains the two laser diodes and the two detector diodes. This dewar offers an excellent alternative to systems with separate detector dewars and helium refrigerator cold heads, especially for field applications.

Infrared light from each of the laser diodes in the dewar is collected by a reflective microscope objective (15×) and focused onto a 200-μm pinhole, which defines the input aperture. This pinhole is used only during alignment, so it is mounted on a removable, kinematically indexed base. The microscope objective is mounted on an *X*-*Y*-*Z* translator to allow accurate focusing into the fixed aperture. Past the input apertures, the two infrared beams are collimated and combined on the main beam splitter. One leg of the beam splitter (the "reference leg") is directed through a gas calibration cell and onto a detector. Light passing through this cell has strong absorption features that are used to identify and lock the spectral line positions. The reference leg also passes through a grating monochromator before being focused onto the detector. The monochromator is useful for identifying the wavelength of the diode during setup of the instrument.

The "signal leg" is directed to a pair of flat mirrors and onto a large gimbal-mounted steering mirror which directs the beam off the table and across the roadway to a corner cube retroreflector. The return beam is collected by the large steering mirror and a curved mirror of similar diameter, passed through several more flat mirrors, and finally focused onto the signal beam detector. An ocular can be dropped into the path of the return beam allowing one to observe and optimize the aim of the outgoing signal beam. While viewing through this ocular, the operator can simultaneously adjust the gimbal-mounted steering mirror to place the image of the corner cube over the ocular's cross hairs. Under many conditions, scattered light from the HeNe "trace laser" (see below) can be seen on the corner cube's gold surface, showing the precise location of the optical beam at the corner cube.

A parallel visible optical system is employed for alignment and setup. A red HeNe "trace" laser beam passes through a dichroic beamsplitter and is coaligned with the infrared beam. Coalignment is guaranteed by focusing the beam through the input aperture. The trace beam is an indispensable aid for alignment of the optical system. In addition, the trace beam is used to accurately calibrate the monochromator, via higher-order diffraction. The fourth port of the dichroic beamsplitter can be used to visibly observe the laser diode. An eyepiece mounted at the position conjugate to the pinhole forms an effective microscope for viewing the laser diode.

1.3 Data processing and analysis techniques

Our data acquisition method is an advanced form of sweep integration carried out by a software package developed at Aerodyne Research. This software uses commercially available data acquisition boards to control and monitor the diode lasers. The software sweeps the laser frequency over the full infrared transition or group of transitions, then integrates the area under the transitions by using nonlinear least-squares fitting to the known spectral line shapes and positions. We do not generally use frequency modulation (FM) techniques because we prefer the clear connection between the direct absorption spectrum and the species' concentration. This data acquisition approach is highly flexible and can be used for many different applications.

There are several advantages to this sweep integration approach. First, absolute species concentrations are returned from the nonlinear least-squares fits so that external calibration is not required. The species concentrations are tied to the absolute spectroscopic data found in the HITRAN data base [26]. Second, the line shape functions are known from theory and can be precisely calculated. Finally, this detailed understanding of the expected line shapes and positions allows one to easily monitor complex and overlapping spectral features. We call this "fingerprint fitting". This is important because monitoring several transitions for one species can enhance sensitivity and is sometimes necessary, especially for larger molecules. In addition, fingerprint fitting allows one to monitor multiple species simultaneously, since we can use overlapping lines, and it even allows one to fit unknown lines which overlap the desired spectrum as a method of removing background absorption from unknown species. This feature is particularly useful in the present application to the analysis of overlapping N_2O and CO_2 lines at atmospheric pressure.

The details of the data acquisition process can be divided into several tasks which we will discuss separately:

1. the software creates a waveform which is used to modulate the frequency of the laser or lasers;
2. the output of the infrared detectors are recorded as a function of time and this data is stored in the computer's extended memory;

3. the program divides the data in extended memory into individual sweeps and averages the individual sweeps to produce one resultant spectrum for each laser;
4. the resultant spectra are analyzed spectroscopically to determine the concentrations or column densities of any species which absorb in that spectral window;
5. the column densities are displayed to the operator, saved to disk, and analyzed to provide emission indices for each of the pollutant species.

The modulation waveform. In the experiments, the laser temperature is held constant while the current through each laser is modulated with a computer-generated saw tooth to sweep the output frequency across the infrared transition. The temperature and base current of each laser diode are fixed by a dual laser controller (Laser Photonics, Inc.). Typical modulation waveforms are shown in Fig. 2. The current is varied linearly for a given time period, which causes a variation of the frequency of the laser light that the diode emits. Then the current is set to a much lower value below the threshold for laser emission. This provides a measurement of the detector output in the absence of laser light. Each laser is below its light-emission threshold while the other is swept. Both lasers are below threshold at the end of the scan.

The digital waveform is converted to an analog voltage at a rate of 300 kHz by a 12-bit digital-to-analog converter (Scientific Solutions, Lab Maser AD). Typically 150 points are used to represent the waveforms so that each frequency sweep is 500 μs in duration.

The infrared detector output. The detector output voltage is sampled by an analog-to-digital converter using the same data acquisition board. The individual spectra are automatically transferred to the computer's extended memory by using direct memory access.

The averaged spectra. The spectra are coaveraged by assembly language averaging routines in order to maintain a 100% duty cycle. For automotive exhaust measurements, the averaging time is typically set to about 10 ms in order to be able to resolve temporal structure in the exhaust plume. The measurement cycle is triggered by a vehicle blocking the optical path. Usually, the laser beam height is chosen to be about 29 cm which is a typical tailpipe height. In fact, the measurement process actually begins before the vehicle blocks the laser beams since the instrument acquires background spectra continuously while waiting for the next vehicle. The exhaust plume spectra are each divided by the most recent background spectrum in order to eliminate the effects of background absorption and to improve sensitivity. This is especially important for carbon dioxide whose background column density in a 20-m path (~ 7000 ppm-m) is nearly as large as the initial column density observed in the exhaust plume with optimal overlap of laser and plume (~ 13 000 ppm-m).

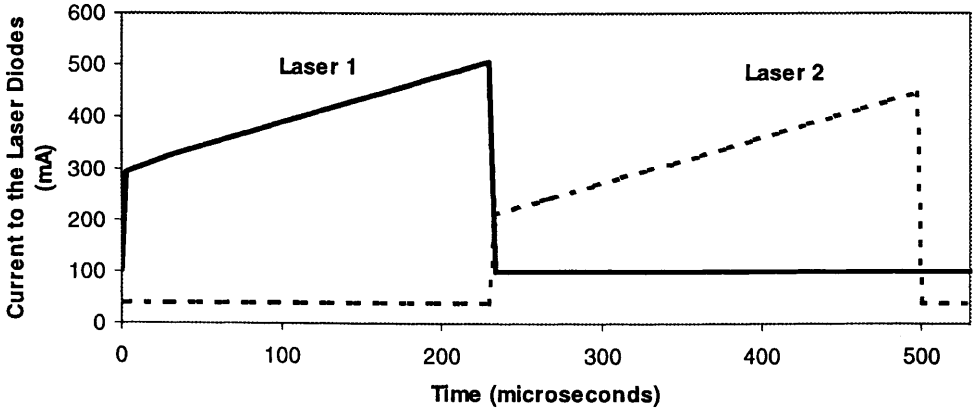

Fig. 2. Sawtooth current input used to modulate the diode laser frequency

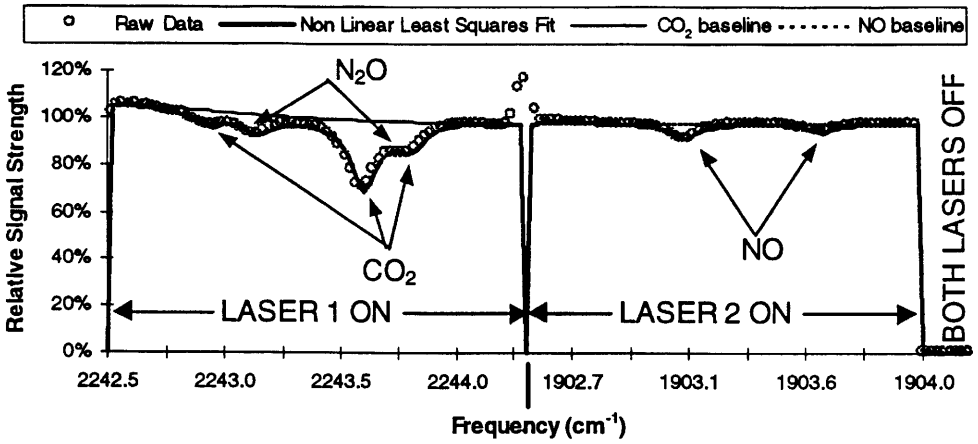

Fig. 3. Two-laser combined-frequency scan. Background absorption in the optical path has been removed by dividing the observed spectra by background spectra. A linear frequency scale is drawn which neglects the slightly nonlinear tuning rates of the two lasers

A pair of background-corrected spectra are shown in Fig. 3. We obtained these spectra during field experiments in the Los Angeles area [27, 28]. These spectra were obtained during the 12.5-ms time slice corresponding to maximum absorption for a plume with an NO concentration of 1400 ppm and an N_2O concentration of 240 ppm. The scan time for each laser was 250 μs; therefore, the laser scans were essentially simultaneous. Twenty-five scans of each laser were co-averaged to give a column density for each species every 12.5 ms. Nitric oxide was measured by recording the change in absorption of individual rotational–vibrational lines at a frequency around 1903 cm^{-1} (5.25 μm). The diode laser was scanned over a spectral region of 1 cm^{-1} by varying the laser current in order to obtain a baseline on either side of a pair of spectral lines. The laser was turned off at the end of each scan to obtain the total laser intensity during the scan. This is particularly important for open-path monitoring through a turbulent atmosphere where the collected laser intensity varies significantly from scan to scan. Carbon dioxide was monitored by using a pair of rovibrational lines at 2243 cm^{-1} (4.45 μm). A pair of nitrous oxide (N_2O) absorption lines were present in the CO_2 scan region and were used to obtain a measurement of the N_2O column density.

Spectral analysis. The resultant spectra were analyzed in real time by using the Levenberg–Marquardt [29] non-linear least-squares method to obtain the best fit to the Voigt line shape and a baseline polynomial. Figure 3 shows the observed spectra, the fits to the observed spectra, and the least-squares fit determination of the unabsorbed laser intensity. The average NO, N_2O, and CO_2 column densities in the laser beam were calculated from the measured fractional absorption by using the tabulated line strengths and pressure broadening coefficients from the HITRAN data base [26]. The software will fit up to four species simultaneously by using up to 45 individual spectral lines per species.

The spectral analysis assumes that the plume temperature and pressure are equal to the ambient temperature and pressure since the plume rapidly equilibrates with the surroundings. The assumption regarding the plume pressure is undoubtedly sound. However, spectra acquired from portions of the plume very near the tail-pipe exit point might have elevated temperatures. If this were the case, we would expect to see systematic curvature in plots of [NO] versus [CO_2]. This effect appears to be small in our studies of light-duty vehicles. In principle, the plume temperature can be determined from the observed spectrum if necessary, since the spectral line widths and relative spectral intensities vary with temperature.

Although, the frequency scale in Fig. 3 is depicted as linear, the tuning rates of the lasers are not actually linear because of the thermal tuning induced by dropping the lasers below threshold. Hence, the tuning rates of the lasers are greatest at the beginning of each sweep and decrease with time, becoming linear asymptotically. For the spectra shown in Fig. 3, the effect is subtle. The software accounts for the nonlinearity even in extreme cases. The expression used to describe the tuning rate is

$$T = C_1 + C_2 \exp(-C_3 t), \tag{2}$$

where T the laser tuning rate, t is time since the laser was turned on, and the C_i are free parameters describing the tuning rate and are determined by using reference spectra in a separate automated analysis.

Typically, plume spectra are acquired for approximately 0.5 s at a rate of 80–100 Hz. The spectra are stored in computer memory and analyzed immediately after the measurement. The analysis requires approximately 1 s with a 133-MHz Pentium processor. Thus, the current TILDAS system is capable of measuring a vehicle every 1.5 s. This time interval would be reduced by using a faster processor. However, it may not be desirable to measure vehicles which are less than 1 s apart, since the emissions from the first vehicle can contaminate the background of the second vehicle, making the measurement less reliable.

Figure 4 shows the column densides of NO, CO_2, and N_2O measured in the wake of a vehicle as a function of time after the vehicle passed. In this case the spectra were acquired at a data rate of 80 samples per second. The correlation of the three species is remarkably good. Measurements performed on vehicles traveling with speeds up to 70 mph have shown very good correlation of the time traces of NO and CO_2 and very stable NO/CO_2 ratios.

Calculation of emission indices. The data processing software uses a linear regression algorithm to determine the NO and N_2O exhaust concentrations for each vehicle. Every point for which the CO_2 column density is larger than a minimum of 1000 ppm-m is used in this algorithm. This is shown in

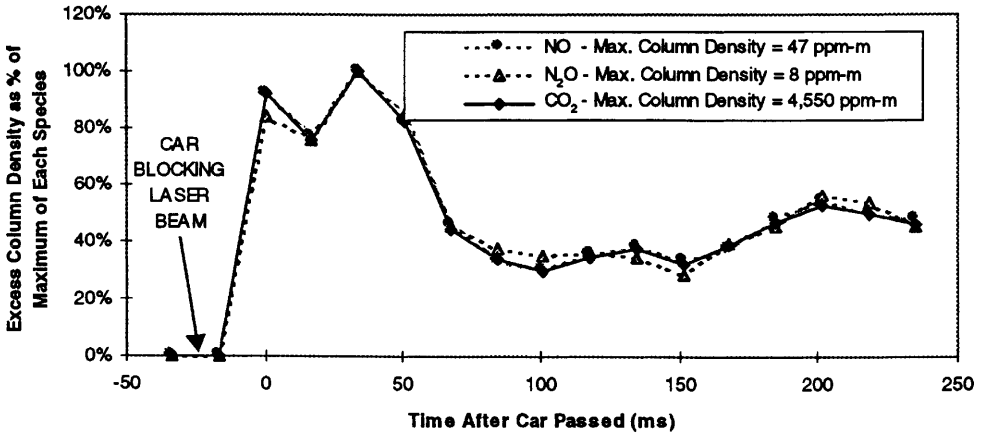

Fig. 4. Column densities of NO, N_2O, and CO_2 in the wake of a vehicle as a function of time

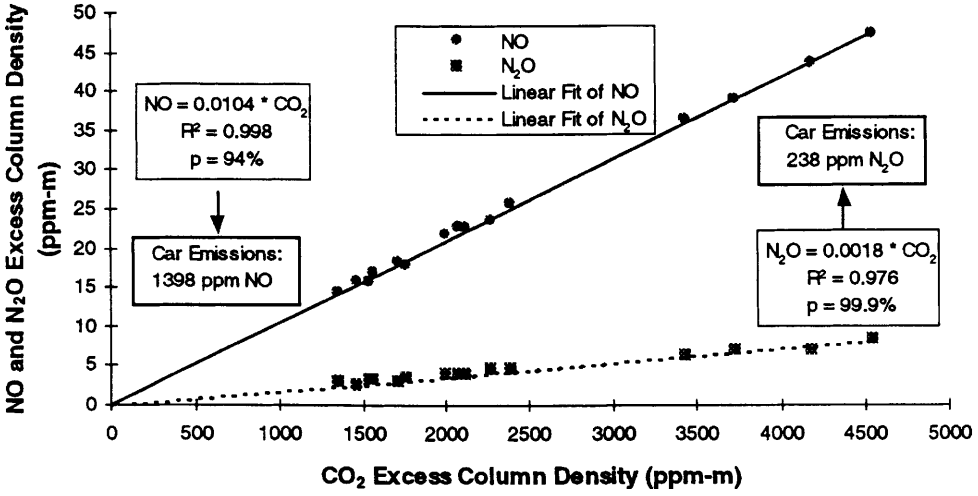

Fig. 5. Regression analysis to determine NO and N_2O emission indices

Fig. 5 for the data from Fig. 4. The obvious correlation between the time dependence of the column densities in Fig. 4 is reflected in the very high values for R^2 from the regression analysis shown in Fig. 5.

1.4 Sensitivity and accuracy of the NO *remote sensor*

The absolute accuracy of the TILDAS instrument is limited by the accuracy of the spectral line parameters from the HITRAN database, which depends on the particular absorption transitions being used. For the NO transitions shown in Fig. 3, this accuracy is estimated at 2%, whereas for the CO_2 transitions in the same figure it is better than 5%. If necessary, better measurements of the absorption parameters can be done with this system, given its very high spectral resolution [29, 30]. Because the accuracy of the instrument is tied to known invariant physical properties, the instrument does not need periodic calibrations. This is a major advantage for field measurements using the TILDAS technique.

The TILDAS instrument detection limit for NO has been estimated from the noise levels observed during open-path field tests performed in the absence of a vehicle. Each measurement was performed for 50 ms to simulate the plume duration of actual on-road exhaust measurements. The observed NO column densities were converted to exhaust mixing ratios by using a value of the CO_2 column density (13 000 ppm-m) that corresponds to the ideal overlap of laser beam and exhaust plume. These tests returned an NO column density near zero with a standard deviation equivalent to an exhaust mixing ratio of $\sim$ 3 ppm. We therefore report the ideal 3σ detection limit as $\sim$ 9 ppm. Experimental confirmation of this detection limit has been obtained by repeated measurements on an ultra-low-emission vehicle (ULEV) as is described below.

This level of sensitivity represents a major breakthrough in NO remote sensing, with an improvement in the detection limit by a factor of approximately 100 over the two widely employed commercial techniques. This enables the TILDAS technique to measure the NO emissions from even the cleanest vehicles on the road.

During the field campaign in the Los Angeles area [27, 28], we performed an experiment which highlights the sensitivity of the TILDAS instrument. The emissions of a prototype ultra-low emission vehicle were measured with the TILDAS remote sensor. This ULEV was made available to us by an automobile manufacturer. This vehicle has been verified by the California Air Resource Board as easily meeting the ULEV emission standard of 0.2 g per mile, which corresponds to an average exhaust concentration of 114 ppm NO based on a fuel economy of 26 mpg. The NO_x emission rate of this vehicle on the Federal Test Procedure (FTP) emissions certification cycle was 0.054 g per mile, which corresponds to an average exhaust concentration of 35 ppm NO. We measured the NO emissions of this vehicle 21 times under a wide variety of driving conditions and always found its emissions to be below the average ULEV emission standard.

These measurements are plotted in Fig. 6 as a function of time, together with a comparison with the full range of NO levels, which can be found in vehicle exhaust. This overview of NO emissions is plotted on the right-hand axis, beginning with the ULEV standard (114 ppm) and extending through the current FTP standard, through a representative NO emission level, and on to an extreme NO emission level which exceeds 3000 ppm. The rest of the figure is referred to the left-hand axis, which spans only the ULEV range (0–120 ppm).

In this part of the figure we plot our measurements of the prototype ULEV. We obtained a mean emission reading of 10 ppm NO, a standard deviation of 18 ppm, and a maximum of 76 ppm. This is consistent with the FTP result. This is the first time that such low emission levels have been successfully measured by remote sensing. We observed two relatively high NO readings taken shortly after the engine had been off for 15 min. We attribute these high readings to a colder catalyst.

The variation in the 21 measurements is a combination of instrumental noise and actual variation in the emissions of the vehicle. There are three points that are significantly higher than the rest and clearly indicate increased NO emissions. If we ignore these three measurements (each of which is greater than 20 ppm), we can use the remaining 18 points to estimate an upper limit to the noise in our emission measurement. These 18 points average 4 ppm of NO with a standard deviation of 5 ppm. This is an upper limit to the instrumental noise for low NO emissions and is consistent with the 3 ppm value for the noise reported above since it is likely that some of the noise in the 18 measurements is due to actual emission variation or nonideal laser-plume overlap.

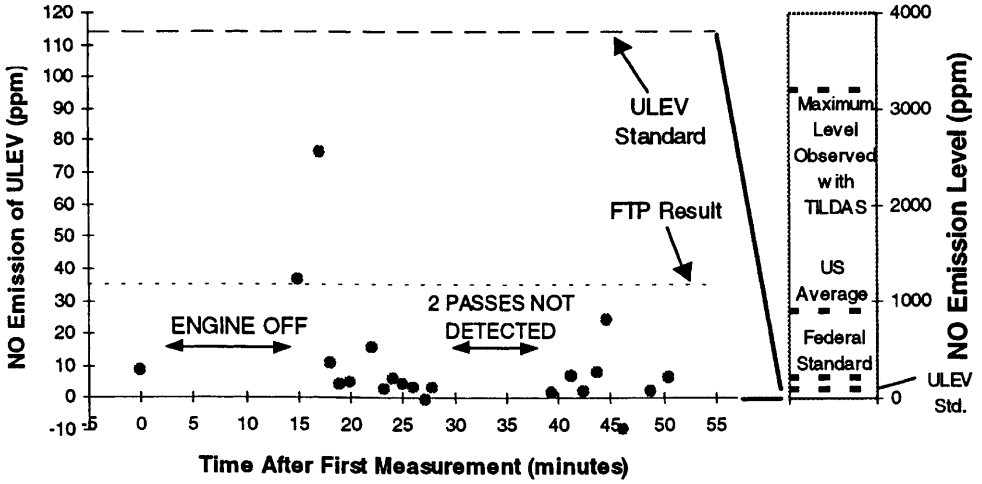

Fig. 6. NO emissions of the ultra-low emission vehicle versus time

It is important to distinguish the detection limit from the measurement precision. The detection limit for NO is the 3σ measurement precision in the limit of low NO column density. In this limit, the dominant noise source is the detection of the NO absorption features. At higher column densities, the quantification of the NO absorption depth will no longer be the dominant source of noise. Other potential noise sources include variations in the width of the laser line, noise in the measurement of the laser intensity returned to the detector, variation of the background NO concentration in the optical path, and variation in the plume temperature or pressure. Typically these effects limit the instrument to a precision of approximately 2%–3% in the measurement of the NO column density even for very high NO concentrations. In addition, there is a similar level of noise in the measurement of the carbon dioxide column density. Both noise sources contribute to the total noise in the NO emission index since the index is calculated as the ratio of the two column densities.

This is highlighted in Fig. 7 where the NO column density is plotted versus the CO_2 column density for two hypothetical measurements (error bars not to scale). As in Fig. 5, the emission index would be the slope of a line going from the origin to the data point in each case. As, can be seen, at low NO/CO_2 ratios the noise in the NO column density measurement dominates the noise in the NO/CO_2 measurement. The 3σ measurement precision will equal the detection limit in this case. In contrast, at high NO/CO_2 ratios the noise in the measurement of the CO_2 column density becomes dominant. For example, if we measure a car emitting 3000 ppm NO, the noise in the NO channel (a few ppm NO) is negligible compared to the noise from the CO_2 channel and other sources, which is equivalent to about 2.5% of 3000 ppm, or 75 ppm NO. In this case the measurement precision is much larger than the detection limit.

A final point is that the measurement precision is also dependent on how well the exhaust plume from the vehicle overlaps with the path of the laser light. Since the noise in the CO_2 and NO column densities is basically independent of the total column density being measured, a lower amount of both gases will result in more measurement uncertainty. In other words, the signal-to-noise ratio is larger for a larger signal since the noise is about constant. This is shown in Fig. 8. For this reason it is preferable to choose remote sensing sites where the vehicles are under significant load, since they will generate a higher volume of exhaust gases, which increases the probability of having a larger signal. But even at a single site each vehicle will be measured with a different precision. Figure 9 illustrates this point by showing the distribution of the signal strengths obtained from the remote sensing of 1500 vehicles in California [27, 28]. We have chosen the maximum value of the CO_2 column density as the surrogate for signal strength (i.e. peak value of the CO_2 curve in Fig. 4). We can see from the figure that a wide range of signal strengths are ob-

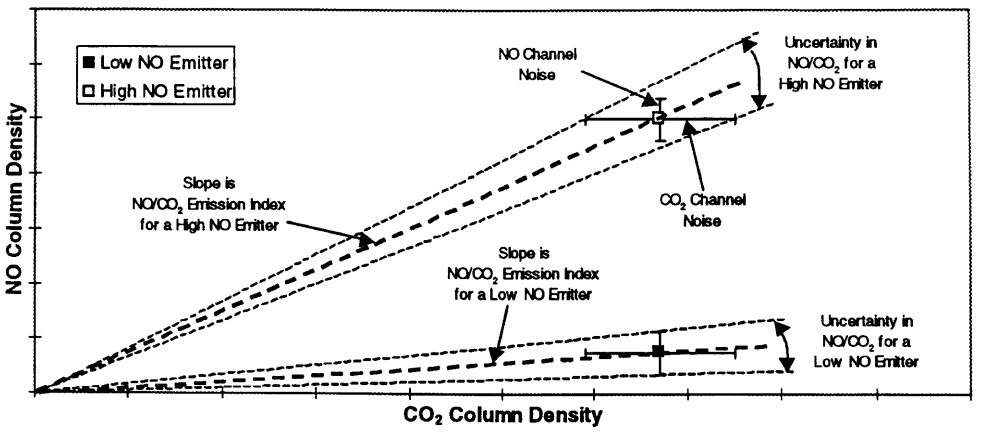

Fig. 7. Effect of the noise in the NO and CO_2 channels on the NO/CO_2 ratio measurement

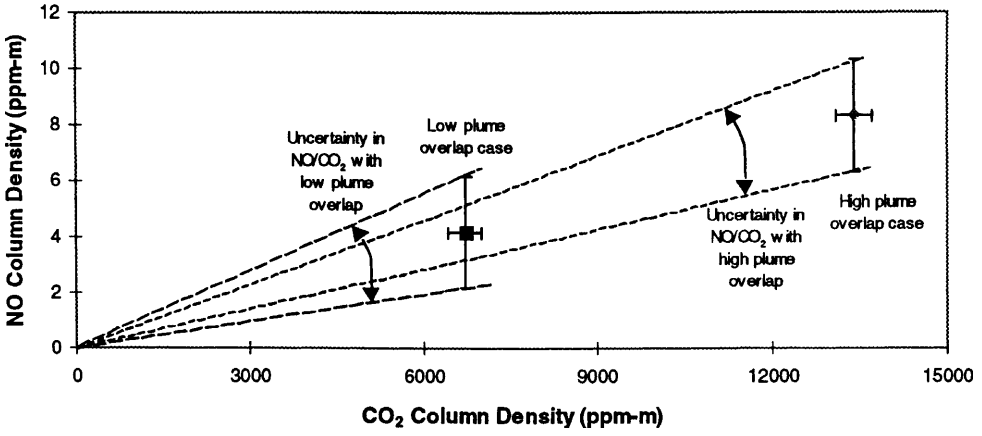

Fig. 8. Effect of plume overlap in the NO/CO_2 measurement noise

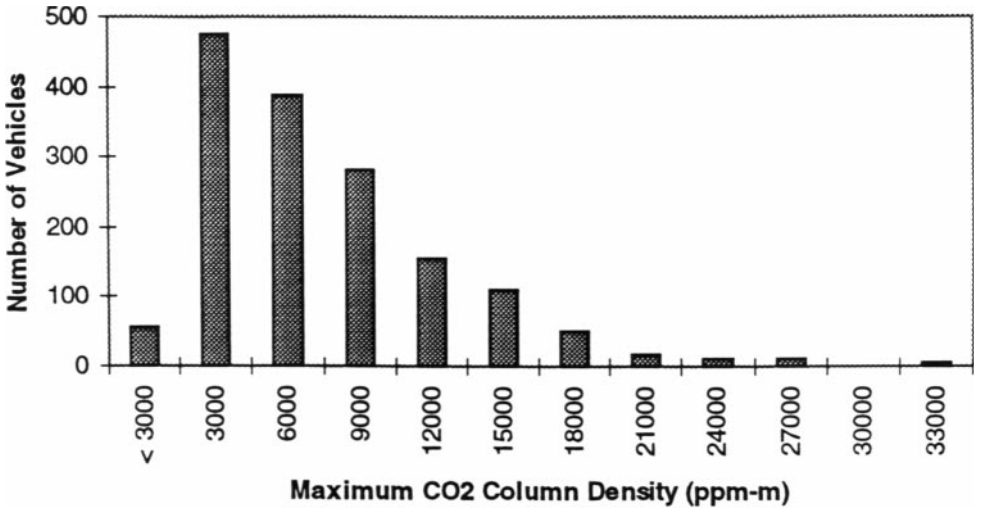

Fig. 9. Distribution of signal strengths in a real-world measurement campaign

served for different vehicles driving through the same remote sensing site.

The points illustrated by Figs. 7–9 are applicable to all remote sensing instruments independent of the particular spectroscopic technology being used.

2 Conclusions

This paper describes the design and testing of our TILDAS-based remote sensing instrument. We have demonstrated that this instrument can detect NO and N_2O emission indices with very high sensitivity under real-world conditions. Furthermore, we have verified that the instrument is highly accurate and requires no field calibration. This is a consequence of the high spectral resolution of the laser sources, which allows absolute column densities to be measured for each of the molecules of interest. There is no significant interference from other species. Long path lengths (> 100 m) can be achieved due to the coherent nature of laser radiation. The system is also capable of measuring CO, NO_2, NH_3, H_2CO, and other small hydrocarbons in vehicle exhaust.

Acknowledgements. The authors of this paper wish to acknowledge the assistance of the following organizations and parties for the support of this research: the National Aeronautics and Space Administration (NASA) for permitting the use in this program of the TILDAS instrument developed by Aerodyne under NASA sponsorship; the US Environmental Protection Agency (EPA) for funding further development of the existing instrument; and the South Coast Air Quality Management District for sponsoring a field measurement campaign in El Segundo, CA.

References

1. National Research Council: *Rethinking the Ozone Problem in Urban and Regional Air Pollution* (National Academy Press, Washington, DC 1991)
2. W.R. Pierson, A.W. Gertler, R.L. Bradow: J. Air Waste Manage. Assoc. **40**, 1495 (1990)
3. N.F. Robinson, W.R. Pierson, A.W. Gertler, J.C. Sagebiel: Atmos. Environ. **30**, 2257 (1996)
4. T.W. Kirchstetter, B.C. Singer, R.A. Harley, G.R. Kendall, W. Chan: Environ. Sci. Technol. **30**, 661 (1996)
5. A.W. Gertler, J.C. Sagebiel, W.A. Dippel, J.A. Gillies, F. Gofa, C.M. O'Connor: Proceedings of the 8th CRC On-Road Vehicle Emissions Workshop, San Diego, California (1998)
6. K.M. Fujita, B.E. Croes, C.L. Benett, D.R. Lawson, F.W. Lurmann, H.H. Main: J. Air Waste Manage. Assoc. **42**, 264 (1997)
7. D.T. Ipps, D. Popejoy: An Updated Verification of the On-Road Vehicle Emission Inventory for the Los Angeles Basin using Ambient Air Quality Data, Proceedings of the 8th CRC On-Road Vehicle Emissions Workshop, San Diego, California (1998)
8. S.H. Cadle, R.A. Gorse, T.C. Belian, D.R. Lawson: J. Air Waste Manage. Assoc. **48**, 174 (1998)
9. S.H. Cadle, R.A. Gorse, T.C. Belian, D.R. Lawson: J. Air Waste Manage. Assoc. **47**, 426 (1997)

10. J.G. Calvert, J.B. Heywood, R.F. Sawyer, J.H. Seinfeld: Science **261**, 37 (1993)
11. S.P. Beaton, G.A. Bishop, Y. Zhang, L.L. Ashbaugh, D.R. Lawson, D.H. Stedman: Science **268**, 991 (1995)
12. G.A. Bishop, J.R. Starkey, A. Ihlenfeldt, W.J. Williams, D.H. Stedman: Anal. Chem. **61**, 671A (1989)
13. R.D. Stephens, S.H. Cadle: J. Air Waste Manage **41**, 39 (1991)
14. M.D. Jack, T.P. Bahan, M.N. Gray, J.L. Hanson, T.L. Heidt, F.A. Huerta, D.R. Nelson, A.J. Paneral, J. Peterson, M. Sullivan, G.C. Polchin, L.H. Rubin, C.B. Tacelli, W.C. Trautfield, R.O. Wageneck, G.A. Walter, J.D. Wills, J.F. Alves, B.A. Berger, J. Brown, J.A. Shelton, G.A. Smith, E.J. Palen, N.W. Sorbo: Society of Automotive Engineers Papers 951943 (1995)
15. Y. Zhang, D.H. Stedman, G.A. Bishop, P.L. Guenther, S.P. Beaton, J.E. Peterson: Environ. Sci. Technol. **21**, 1885 (1993)
16. S.H. Cadle, R.D. Stephens: Environ. Sci. Technol. **28**, 258A (1994)
17. Y. Yang, D.H. Stedman, G.A. Bishop, S.P. Beaton, P.L. Guenther, I.F. McVey: J. Air Waste Manage. Assoc. **46**, 25 (1996)
18. P.J. Popp, G.A. Bishop, D.H. Stedman: Development of a High-Speed Ultraviolet Spectrophotometer Capable of Real-Time NO and Aromatic Hydrocarbon Detection in Vehicle Exhaust, Proceedings of the 7th CRC On-Road Vehicle Emissions Workshop, San Diego, California (1997)
19. G. Sachse, P. LeBel, M. Rana, T. Steele: Application of a New Gas Correlation Sensor to Remote Vehicular Exhaust Measurements, Proceedings of the 8th CRC On-Road Vehicle Emissions Workshop, San Diego, California (1998)
20. C.E. Kolb, J.C. Wormhoudt, M.S. Zahniser, "Recent advances in spectroscopic instrumentation for measuring stable gases in the natural envionment", In: *Biogenic Trace Gases: Measuring Emissions from Soil and Water*, ed. by P.A. Matson, R.C. Harriss (Blackwell Science, Oxford, UK 1995)
21. R.T. Ku, E.D. Hinkley, J.O. Sample: Appl. Opt. **14**, 854 (1975)
22. J. Wormhoudt, M.S. Zahniser, D.D. Nelson, J.B. McManus, R.C. Miake-Lye, C.E. Kolb: SPIE Proc. **2122**, 49 (1994)
23. J. Wormhoudt, M.S. Zahniser, D.D. Nelson, J.B. McManus, R.C. Miake-Lye, C.E. Kolb: SPIE Proc. **2546**, 552 (1995)
24. B.C. Singer, R.A. Harley.: J. Air Waste Manage. Assoc. **46**, 581 (1996)
25. G. Bishop, D.H. Stedman: Acc. Chem. Res. **29**, 489 (1996)
26. L.S. Rothman, R.R. Gamache, R.H. Tipping, C.P. Rinsland, M.A.H. Smith, D.C. Benner, Malathy Devi, J.-M. Flaud, C. Camy-Peyret, A. Perrin, A. Goldman, S.T. Massie, L.R. Brown, R.A. Toth: J. Quant. Spectrosc. Radiat. Transfer **48**, 469 (1992)
27. J.L. Jimenez, D.D. Nelson, M.S. Zahniser, J.B. McManus, C.E. Kolb, M.D. Koplow, S.E. Schmidt: Remote Sensing Measurements of On-Road Vehicle Nitric Oxide Emissions and of an Important Greenhouse Gas: Nitrous Oxide, Proceedings of the 7th CRC On-Road Vehicle Emissions Workshop, San Diego, California (1997)
28. M.D. Koplow, J.L. Jimenez, D.D. Nelson, S.E. Schmidt: Characterization of On-Road Vehicle NO Emissions by Means of a TILDAS Remote Sensing Instrument. Proceedings of the 7th CRC On-Road Vehicle Emissions Workshop, San Diego, California (1997)
29. W.H. Press, S.A. Teukolsky, W.T. Vetterling, B.P. Flannery: *Numerical Recipes in FORTRAN* (Cambridge University Press, New York 1992)
30. J.H. Shorter, D.D. Nelson, M.S. Zahniser: J. Chem. Soc., Faraday Trans. **93**, 2933 (1997)
31. D.D. Nelson, M.S. Zahniser: J. Molec. Spectrosc. **166**, 273 (1994)